PASJ: Publ. Astron. Soc. Japan **47**, L5–L9 (1995)

ASCA Observations of the Spectrum of the X-Ray Background

Keith C. GENDREAU,[1] Richard MUSHOTZKY,[3] Andrew C. FABIAN,[2] Stephen S. HOLT,[3]
Tsuneo KII,[4] Peter J. SERLEMITSOS,[3] Yasushi OGASAKA,[4] Yasuo TANAKA,[4]
Marshall W. BAUTZ,[1] Yasushi FUKAZAWA,[5] Yoshitaka ISHISAKI,[5] Yoshiki KOHMURA,[5]
Kazuo MAKISHIMA,[5] Makoto TASHIRO,[5] Yoshiyuki TSUSAKA,[6] Hideyo KUNIEDA,[6]
George R. RICKER,[1] and Roland K. VANDERSPEK[1]

[1]*Center For Space Research, Massachusetts Institute of Technology Cambridge, MA, 02139 U.S.A.*
[2]*Institute of Astronomy, University of Cambridge, Maddingley Road, Cambridge, CB3 OHA U.K.*
[3]*NASA/Goddard Space Flight Center, Greenbelt, MD, 20771 U.S.A.*
[4]*Institute of Space and Astronautical Science, 1-1 Yoshinodai 3-chome, Sagamihara, Kanagawa 229*
[5]*Department of Physics, School of Science, University of Tokyo, Bunkyo-ku, Tokyo 113*
[6]*Department of Physics, School of Science, Nagoya University, Furo-cho, Chikusa-ku, Nagoya 464-01*

(Received 1994 March 1; accepted 1995 January 20)

Abstract

We present initial results from ASCA on the spectrum of the Cosmic X-ray Background from 0.4 to 10 keV. About 250 ks of deep survey data has been collected from the performance verification phase of ASCA. About 110 ks of dark-earth data are used to assess the internal background. A single power-law describes the X-ray background very well in the 1 to 10 keV with no evidence for a steepening in the 1 to 3 keV range. At 1 keV, the intensity of the X-ray background is 9.6 keV s^{-1} cm^{-2} sr^{-1} keV^{-1}. Our data clearly show an excess above the extrapolation of the single power law model below 1 keV. At least part of this excess can be accounted for with a thermal component as there is evidence for O VII and O VIII emission.

Key words: Cosmology: diffuse radiation — Cosmology: observations — Galaxies: active — ISM: abundances — ISM: bubbles — X-rays: general

1. Introduction

The origin of the X-Ray Background (XRB) remains an important astronomical puzzle (see Fabian, Barcons 1992 for a recent review). A major handle for studying the XRB is its spectrum, which has a 40-keV bremsstrahlung-like shape (Marshall et al. 1980). In the 3–10 keV band this is flat and can be approximated by a power-law of photon index $\Gamma = 1.4$. At lower energies it appears to steepen, in part due to Galactic emission (see McCammon, Sanders 1990; Snowden et al. 1990). It has also been claimed that the extragalactic background has a steep excess intensity below 2 keV (Shanks et al. 1991; Hasinger et al. 1993). Here we use ASCA to determine the spectrum of the XRB over the entire 0.4–10 keV band for the first time.

This band, which covers the transition between the soft and harder bands studied separately before, is very important since most observed extragalactic sources have spectra that are steeper than the XRB itself and so are expected to create a soft excess. The energy at which this excess dominates the XRB indicates the mean spectral index and contribution of these sources. While such steep sources may contribute heavily to the soft XRB, the most plausible current models for the harder XRB invoke a population of absorbed or reflection sources (Setti, Woltjer 1989; Morisawa et al. 1990; Fabian et al. 1990; Terasawa 1991; Madau et al. 1993; Zdziarski et al. 1993). A high density of absorbed sources is also inferred from a comparison of the source counts in the soft and hard X-ray bands (Warwick, Stewart 1989; Hayashida 1990; Hasinger et al. 1993).

2. The X-Ray Data: Cosmic

We have accumulated a 250 ks exposure spectrum of the XRB in each of the Solid State Imaging Spectrometers (SIS) (Bautz et al. 1995 in preparation). The data come from deep exposures of the Draco, North Ecliptic Pole, Lockman Hole, and Lynx fields observed during the performance verification phase. We used 4-CCD faint and bright observation mode data in this study. The separate observations of these fields will be described elsewhere by the ASCA PV team. Each field has a galactic latitude near 45° and thus a low galactic absorption in

the SIS energy band (0.4–12 keV). The largest H I column density in these fields is about 6×10^{20} cm^{-2} (Stark et al. 1992). The data have been carefully selected to minimize the effects of optical light leakage and solar scattered X-rays by taking data when the earth elevation angle (the angle between the telescope field of view and the Earth's limb) was greater than 30°. In addition, parameters which are particularly sensitive to optical light leakage, the number of CCD pixels above threshold and the number of detected events, including cosmic rays and hot pixels, per integration were used to make an additional selection condition. Cut-off values for these parameters were made after inspecting the light curves. Data taken near the SAA are also avoided. With these criteria data collected during satellite night and satellite day appear comparable and were combined to yield the total exposure time. The CCDs have some bad pixels with excess dark current. Some of these pixels appear as events 100% of the time and are called "hot pixels," while others turn on less frequently and are called "flickering pixels." Pixels which turned on at least twice during any exposure were rejected.

3. The X-Ray Data: Internal

In the SIS, approximately 98% of the cosmic ray induced events can be rejected by grade which is a measure of the event shape. We have selected data with grades 0 through 4 (Bautz et al. 1995 in preparation) for our X-ray analysis. To handle the remaining 2% of the internal background, data were collected while ASCA looked at the dark side of the earth. 110 ks of dark-earth data were collected from 1993 April to September during satellite night with the same SIS data selection criteria as were used for the sky data . Flickering pixel removal was done as it was for the sky data. Finally, a slight dependence on the local magnetic rigidity was observed in the dark earth data. Therefore, both the sky data and the dark earth data were selected when the rigidity was greater than 8 GeV c^{-1}. The spectrum can be characterized by a nearly flat continuum, fitted without using the telescope and detector responses, with fluorescence lines due to iron, nickel, aluminum, silicon, and gold. There is also an oxygen line present, which we consider to be most likely of atmospheric origin since there is no Si–K line of comparable strength seen in the spectrum while the fluorescence yield of oxygen is more than an order of magnitude smaller than that of silicon and there is much more silicon around the sensitive part of the detector. The sky data probably does not have this oxygen line, since the earth elevation angle cut is so stringent. The removal of the oxygen line from the internal background spectrum does not affect the results. The average spectrum of the dark-earth data set from the two SIS sensors has a total intensity of 7.3×10^{-4} ct s^{-1} keV^{-1} per CCD (6×10^{-4} ct s^{-1} keV^{-1}cm^{-2}). There is a difference of about 12% between the two independent SIS detectors on ASCA. A more detailed study of the internal background is presented elsewhere (Gendreau et al. 1994). This spectrum was fitted and used as a background model for the sky spectrum (figure 1).

Table 1. Fitting results of the hard XRB with the SIS over different band passes.

Band pass	$\Gamma_{\rm hard}$	$Norm_{\rm hard}$ keV s^{-1} cm^{-2} sr^{-1} keV^{-1}
3–7 keV	1.38 ± 0.12	8.5 ± 3.0
1–3 keV	1.33 ± 0.05	8.6 ± 0.4

4. The XRT Response

While the response of the SIS has very little dependence on the source angular distribution, the X-ray telescope (XRT) response to an extended source is different than it is for a point source primarily due to stray X-rays which reflect off of the telescope surfaces only once (Serlemitsos et al. 1995). For each energy from 300 eV to 12 keV, in 100 eV steps, 10^7 photons with incident angles randomly distributed between 0° and 2° of the XRT optical axis were ray traced through the XRT model. Photons landing within the regions occupied by each of the 8 individual CCDs of each SIS were counted and normalized to the incident surface brightness to yield an XRT throughput in units of [sr cm^2].

5. Fitting Results

In all the fitting, cosmic components are added to the independently-fitted internal model (from the dark earth data) and the C-statistic is minimized (Cash 1979). Data above 7 keV where the internal background becomes comparable to the sky background were excluded. Also, a 500 eV wide region around a known, but uncalibrated instrumental feature at 2 keV is ignored.

In the 1–7 keV band, we find that a power law of photon index of 1.41 ± 0.03 and normalization of 8.9 ± 0.4 keV s^{-1} cm^{-2} sr^{-1} keV^{-1} at 1 keV can describe the data (reduced $\chi^2 = 1.8$ for 256 d.o.f.). To check the robustness of the single power law fit, we divided this band into several overlapping bands and fit a power law separately (table 1). Individual fits with each of the eight CCDs of the two SIS detectors over the 1–7 keV band yield a mean power law index of 1.43 ± 0.09 and mean normalization 8.9 ± 0.8 keV s^{-1} cm^{-2} sr^{-1} keV^{-1} at 1 keV. No individual fit is greater than 2σ away from the mean result. The individual fits are much better (re-

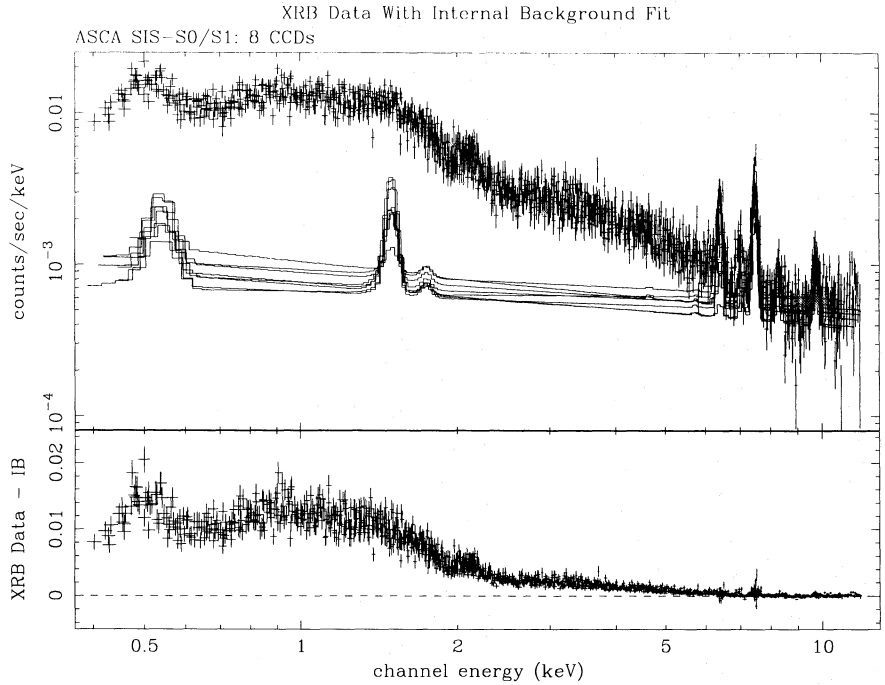

Fig. 1. Spectrum of the XRB obtained with the eight CCDs of the SIS detectors. The total exposure time is approximately 250 ks. The models drawn in the upper panel are the results of analytical fits to the dark-earth data spectrum for each of the 8 CCDs. The instrumental background contains emission lines due to aluminum, nickel, iron, and gold on top of a continuum. The lower panel shows the XRB data with the internal background models subtracted.

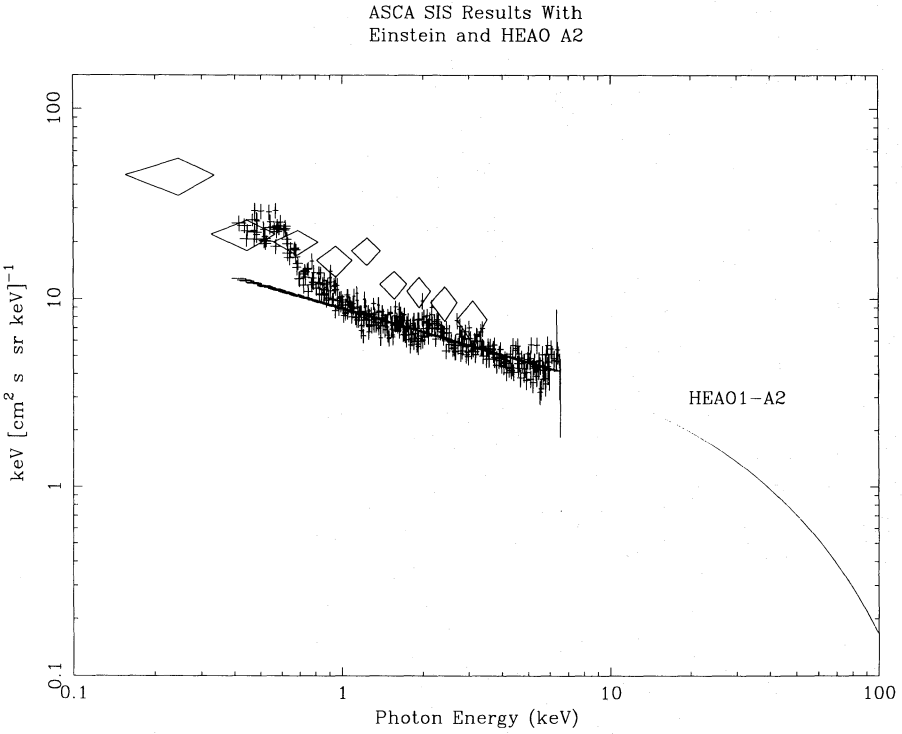

Fig. 2. The unfolded spectrum of the XRB from 0.4 to 7 keV with the best fit model for the 1–7 keV band: a single power law of photon index 1.41 and normalization 8.9 keV s^{-1} $cm^{-2}sr^{-1}$ keV^{-1} at 1 keV. The excess above the model below 1 keV is due, in part, to galactic emission. Also shown are the Einstein satellite IPC results (Wu et al. 1991) as diamonds and the HEAO1-A2 result (Marshall et al. 1980).

duced $\chi^2 = 1.37$) than the combined fit which may reflect intrinsic fluctuations in the sky. As an independent check of this result, we make use of the Gas Imaging Spectrometers (GIS) also flying on ASCA. From the GIS detectors, we obtain the same result that a single power law component of index about 1.4 describes the 1–10 keV data well.

Next, we consider the full SIS energy range down to the 0.4 keV. The discrepancy between the high energy XRB model and the low energy data is quite clearly seen in the residuals below 1 keV (figure 2).

As a first attempt to explain the excess, a Raymond-Smith thermal component was added to the hard power-law. Constraining the metal abundance of the plasma to be cosmic, we obtain a temperature of 0.147 ± 0.006 keV, $\Gamma_{\rm hard} = 1.47 \pm 0.02$, and $Norm_{\rm hard} = 9.4 \pm 0.4$ keV s^{-1} cm^{-2} sr^{-1} keV^{-1}. The reduced $\chi^2 = 2.1$ for this model. Removing the constraint on the abundance, we improve the fit (Δ likelihood = 86, reduced $\chi^2 = 1.8$) and obtain an abundance of 0.04 ± 0.01, a temperature of 0.165 ± 0.006 keV, $\Gamma_{\rm hard} = 1.41 \pm 0.02$, and $Norm_{\rm hard} = 9.0 \pm 0.4$ keV s^{-1} cm^{-2} sr^{-1} keV^{-1}. Since this low abundance may be implausible for the Galaxy, we have added a second power-law component, while fixing the thermal component's abundance to be cosmic. The best fit (reduced $\chi^2 = 1.8$) with this model had a temperature of $kT = 0.16 \pm 0.01$ keV, $\Gamma_{\rm hard} = 1.37 \pm 0.05$, $Norm_{\rm hard} = 8.4 \pm 0.5$ keV s^{-1} cm^{-2} sr^{-1} keV^{-1}, $\Gamma_{\rm soft} = 3.9 \pm 0.7$, $Norm_{\rm soft} = 1.0 \pm 0.7$ keV s^{-1} cm^{-2} sr^{-1} keV^{-1}. The dominant features in this model are the O VII and O VIII lines at 574 and 650 eV.

We also tried replacing the soft power law with a bremsstrahlung component. The best fit (reduced $\chi^2 = 1.8$) for the bremsstrahlung component had a temperature of $kT = 0.24$ keV while the Raymond Smith component had a temperature of $kT = 0.15$ keV and the hard power law had a photon index of 1.39 and normalization of 8.7 keV s^{-1} cm^{-2} sr^{-1} keV^{-1}.

Over our bandpass, the continuum component of all the models we have tried is well approximated by a soft power law. A model which describes the data as well as the best thermal plasma plus power law model is a double power law with lines added at 574 and 650 eV. The best fit parameters for this model were $\Gamma_{\rm hard} = 1.4$ (fixed), $Norm_{\rm hard} = 8.4 \pm 0.2$ keV s^{-1} cm^{-2} sr^{-1} keV^{-1}, $\Gamma_{\rm soft} = 4.0 \pm 0.2$, $Norm_{\rm soft} = 1.3 \pm 0.3$ keV s^{-1} cm^{-2} sr^{-1} keV^{-1}, 0.574 keV line intensity $= 2.3 \pm 0.3$ photon s^{-1} sr^{-1} cm^{-2}, and 0.65 keV line intensity $= 0.6 \pm 0.15$ photon s^{-1} sr^{-1} cm^{-2}. Since the quoted errors indicate the 90% confidence ranges for the parameters, the line detections are highly significant.

The best fit double power law (without lines) had $\Gamma_{\rm hard} = 1.24$, $Norm_{\rm hard} = 6.9$ keV s^{-1} cm^{-2} sr^{-1} keV^{-1}, $\Gamma_{\rm soft} = 3.5$, $Norm_{\rm soft} = 2.9$ keV s^{-1} cm^{-2} sr^{-1} keV^{-1} and a reduced $\chi^2 = 2.7$.

ROSAT and Einstein data (Hasinger et al. 1993; Wu et al. 1991) suggest that the X-ray background steepens in the 2 to 3 keV range. Recent ROSAT results resolve out about 60% of the X-ray background at 1 keV into sources with an average photon index of 2.1–2.2. With ASCA, we find that a single power law of photon index near 1.4 fits well in the 1–7 keV range. To address this discrepancy, we have tried to see how large a contribution a soft power law component could make to the X-ray background at 1 keV. Without any constraints on the hard power law component, the 90% confidence upper limits to the contributions of soft power law components with indices $\Gamma_{\rm soft} = 1.7$, 2.0, 2.5, and 3.0 are 94%, 71%, 43%, and 26%, respectively, of the XRB at 1 keV. However, at these limits, the hard power law is forced to be much harder than $\Gamma_{\rm hard} = 1.4$. Constraining the hard power law component to have an index $\Gamma_{\rm hard} = 1.4$, the 90% confidence upper limits to the contributions of soft power law components with indices $\Gamma_{\rm soft} = 1.7$, 2.0, 2.5, and 3.0 are 38%, 23%, 18%, and 16%, respectively, of the XRB at 1 keV.

6. Conclusions

ASCA confirms the well-established power-law slope of the XRB in the 2–10 keV band. A new result from ASCA is that there is no steepening of this power law in the 1–3 keV range. Thus a single power law with index of about 1.4 fits the entire 1–10 keV range. BBXRT obtained a similar result with much less statistics (Jahoda et al. 1992). This component is most likely the result of many individual sources — mostly AGN (Fabian, Barcons 1992; and references within). ASCA has seen many absorbed sources with hard spectra (for example, see Fukazawa et al. 1994) which may add up to make the observed spectrum.

Below 1 keV, we see an excess which is due in part to the hot interstellar medium in which the solar system resides (Tanaka, Bleeker 1977; Inoue et al. 1979; Cox 1987; McCammon et al. 1990). With ASCA we find a plasma with a temperature of about 0.16 keV which is approximately consistent with earlier sounding rocket flights and ROSAT results (Inoue et al. 1979; McCammon et al. 1990; Hasinger 1992; Snowden et al. 1990). We find that the addition of a soft power-law with slope similar to the continuum of the thermal component allows us to vary the abundance of the thermal component while maintaining a good fit, since the equivalent width of the oxygen lines against the thermal continuum is a measure of the abundance. Perhaps the soft power law is a result of the summation of many individual sources as suggested by recent ROSAT results (Hasinger 1992). However, the soft power-law is much steeper than would be expected from AGN (Hasinger et al. 1993). Alternately, it may

be the case that the low abundance of the single power-law plus thermal component model reflect some state of non-equilibrium of the local interstellar plasma.

We thank all the instrument and operation teams that made ASCA a success. Also, we thank Dan McCammon for useful discussions. This work was supported by NASA grant NASW-4372.

References

Cash W. 1979, ApJ 228, 939
Fabian A.C., Barcons X. 1992, ARA&A 30, 429
Fabian A.C., George I.M., Miyoshi S., Rees M.J. 1990, MNRAS 242, 14P
Fukazawa Y. et al. 1994, PASJ 46, L55
Gendreau K. 1994, ASCA News, No 2, 5
Hasinger G. 1992, in The X-Ray Background, ed X. Barcons, A.C. Fabian (Cambridge University Press, Cambridge) p229
Hasinger G., Burg R., Giacconi R., Hartner G., Schmidt M., Trümper J., Zamorani G., 1993, A&A 275, 1
Hayashida K. 1990, PhD thesis, University of Tokyo
Inoue H., Koyama K., Matsuoka M., Ohashi T., Tanaka Y., Tsunemi H. 1979, ApJ 227, L85
Jahoda K. et al. 1992, in The X-Ray Background, ed X. Barcons, A.C. Fabian (Cambridge University Press, Cambridge) p240
Madau P., Ghisellini G., Fabian A.C. 1993, ApJL 410, L7
Marshall F.E., Boldt E.A., Holt S.S., Miller R.B., Mushotzky R.F., Rose L.A., Rothschild R.E., Serlemitsos P.J. 1980, ApJ 235, 4
McCammon D., Sanders W.T. 1990, ARA&A 28, 657
Morisawa K., Matsuoka M., Takahara F., Piro L. 1990, A&A 236, 299
Setti G., Woltjer L. 1989 A&A 224, L21
Shanks T., Georgantopoulos I., Stewart G.C., Pounds K.A., Boyle B.J., Griffiths R.E. 1991, Nature 353, 315
Serlemitsos P.J., Jalota L., Soong Y., Kunieda H., Tawara Y., Tsusaka Y., Suzuki H., Sakima Y. et al. 1995, PASJ 47, 105
Snowden S.L., Cox D.P., McCammon D., Sanders W.T. 1990, ApJ 354, 211
Stark A.A., Gammie C.F., Wilson R.W., Bally J., Linke R.A., Heiles C., Hurwitz M. 1992, ApJS 79, 77
Tanaka Y., Bleeker J.A.M. 1977, Space Sci. Rev. 20, 815
Terasawa N. 1991, ApJL 378, L11
Warwick R.S., Stewart G.C. 1989, in X-Ray Astronomy, 2. AGN and the X-Ray Background (ESA SP-296, Noordwijk) p727
Wu X., Hamilton T., Helfand D.J., Wang Q. 1991, ApJ 379, 564
Zdziarski A., Zycki P.T., Svensson R., Boldt E. 1993, ApJ 405, 125